https://dx.doi.org/10.22161/ijaers.4.5.7 *ISSN: 2349-6495(P) | 2456-1908(O)*

Numerical Investigation of a Naca Air Intake for a Canard Type Aircraft

B.H. da Silveira, P.R.C. Souza, O. Almeida

Experimental Aerodynamics Research Center, Federal University of Uberlandia, Uberlandia, Brazil

Abstract*—The present work aims to investigate the implementation of a new air intake on a canard type aircraft, through efficiency and drag calculations using a commercial CFD code. Preliminary semi-empirical studies proved that the NACA air inlet was the best option available since it reduces aerodynamic drag. Later, a set of numerical studies were performed with the air intake mounted on a flat plate (theory check) and in the aircraft's fuselage, in order to check the effect of the incoming flow disturbed by the fuselage. These simulations were performed using Reynolds-averaged Navier-Stokes (RANS) and turbulence modeling. Data analyses were based on the air inlets efficiency, drag, velocity profiles and the effect of the fuselage's curvature. The results confirmed that the NACA air intake has satisfactory performance, especially in reducing drag, and led to further considerations about the design of the aircraft in terms of sizing the air intakes. Also, the approach applied in this work was considered to be a methodology for new design implementation and/or selection. The CFD results have been corroborated by an empirical approach from the ESDU (Engineering Science Database Unit). This study was part of collaboration between the Brazilian Aircraft Factory (FABE) and the Federal University of Uberlândia (UFU).*

Keywords*—*Air inlet, Aerodynamic drag, Efficiency, CFD, Naca.

I. INTRODUCTION

For the operation of several systems on an aircraft, as air conditioning, auxiliary turbines, ventilation and engine, it is necessary acquisition of outside air. This capture is only possible through the existence of air inlets. When discussing the construction of a gas turbine engine, understanding the function of the inlet is rather important since it has a great impact on engine performance, improving the entire aircraft. It is also possible to see other applications for refrigeration and other cooling systems, for instance. For aeronautical application, it may be identified at least two types of air intakes: NACA and scoop.

The NACA duct, have no external projections, as shown in Fig. 1, resulting in low aerodynamic drag and do not require specific structural reinforcements, causing no impact on the weight of aircraft. However, this type of air intake is generally less efficient than a scoop inlet because most of the incoming flow is from the boundary layer which develops upstream of the inlet. Its operation is based on the deviation of the air flow into the throat of the air inlet, this deviation caused by the diverging slope and by the generation of vortices in their side walls.

Fig.1: NACA air inlet – J-HangarSpace, 2015.

Whereas the scoop air inlets, which appear in Fig. 2, are external projections designed to capture air outside the boundary layer, thereby recovering higher dynamic pressure and leading to a higher efficiency. The major disadvantage of this type of installation in relation to NACA intakes is the amount of aerodynamic drag, which causes weight gain and affects the aerodynamic performance of aircraft flight. Another disadvantage is the ingestion of liquids (water), foreign objects and the formation of ice.

Fig.2: Scoop air inlet – Kerbal Space Program, 2013.

The majority of the recent studies use CFD techniques for analysis and experimentation of air inlets for different types of application (Taskinoglu, et. al, 2002), both in conditions of supersonic and subsonic flow. For the type of air inlet concerned, there are several techniques to

https://dx.doi.org/10.22161/ijaers.4.5.7 *ISSN: 2349-6495(P) | 2456-1908(O)*

improve performance and efficiency. It can be cited, pulsating jets, vortex generators, flow deflectors and optimization of geometrical parameters (Rodriguez, 2000).

Traditionally in order to evaluate the performance of the air inlets features three parameters. The first is mass flow of air which enters the air intake or more precisely, the ratio between this mass flow and the theoretical mass flow that would enter under conditions of undisturbed flow. The second is the dynamic pressure recovery efficiency of the entry, which is defined as the ratio between the dynamic pressure in the throat of the inlet and dynamic pressure in the undisturbed flow. The last one is the drag coefficient at the entrance.

Currently, one of the resources for which it has sought to increase the efficiency of air inlet type NACA is the use of vortex generators (de Faria and Oliveira, 2002). In particular, some Boeing 737's have this kind of inlet for feeding the Auxiliary Power Unit (APU) located in the tail. However, very little, information is available in the open literature about the influence of the main geometric parameters which determine efficiency and drag curves of these types of air inlets.

What is accessible related to conventional air inlets is published in Engineering Sciences Data Unit, ESDU (item n° 86002, 1986).This database possess several studies which conclude that dynamic pressure recovery efficiency is strongly influenced by variations in mass flow, increasing thickness of the boundary layer results in low efficiency and a uniform and continuous flow at the entrance of the throat.

The focus of this paper is to analyze the variation of the NACA inlet efficiency, using Computational Fluid Dynamics (CFD) for obtaining the results to a canard type aircraft. A set of numerical studies were performed with the air intakes mounted on a flat plate (theory check) and in the aircraft's fuselage. These simulations were performed using Reynolds-averaged Navier-Stokes (RANS) simulations conducted by the well-known CFD ++ commercial code from MetacompInc®. An analysis based on the air inlets efficiency, drag, velocity profiles and the effect of the fuselage's curvature are detailed in the following sections in order to evaluate the implementation feasibility of this component for a canard-type aircraft.

II. CASE STUDY – CANARD TYPE AIRCRAFT

The actual application or namely a case study is a general aviation aircraft classified in the experimental category called Bumerangue EX-27. The Bumerangue EX-27 Crosscountry is a quadriplace aircraft, monoplane, single engine installed in the pusher configuration, namely a canard configuration, with retractable landing gear and closed cabin with two access doors in the front. The fuselage is built with composite (fiberglass) with epoxy resin laminated through vacuum process as usually employed in aeronautical construction. All fixation points are constituted by stainless steel 304 according to the imposed strength limits. The rudders and canard are also made by fiberglass. The powerplant system is composed by a Continental TSIO 360 EB Turbo – air refrigerated developing 210HP at 2700 rpm and equipped with a MT propeller with stainless steel protection and fiberglass. The whole wing is one piece of fiberglass and all fixation parts also received chemical treatment against corrosion and electrostatic paint.

Fig. 3 provides an overview about the Bumerangue EX-27 Crosscountry aircraft. As this aircraft is powered in a pusher configuration, the engine is installed at the back of the aircraft and requires special attention in terms of cooling (air ventilation). In order to guarantee the right air flow through the engine compartment additional air inlets must be placed at the rear end of the aircraft. The options are scoops and NACA air inlets which have been addressed in this work. As mentioned before, the approach is to select an air intake that could supply the air requirement for the engine compartment with a minimum penalty on drag for the whole aircraft. Thus, the main goal is to see if the NACA intake could comply with such requirements.

Fig.3: Bumerangue EX-27 Cross-Country airplane (courtesy from FABE LTD.).

III. EMPIRICAL METHOD

Previous calculations for sizing a NACA air intake for the airplane have been performed with the use of a well-known semi-empirical method, namely, ESDU (Engineering Science Database Unit) – ESDU (1986). To predict and calculate the parameters from the flush inlet (NACA) – Fig. 4 – this semi-empirical method utilizes a catalogued database to compute the drag and pressure recovery of small auxiliary air inlets totally or partially immersed in the boundary layer. This approach is suitable at subsonic speeds. Essentially, the theory of two-

https://dx.doi.org/10.22161/ijaers.4.5.7 *ISSN: 2349-6495(P) | 2456-1908(O)*

dimensional boundary-layer calculation is used as reference and modified in the light of the available experimental data.

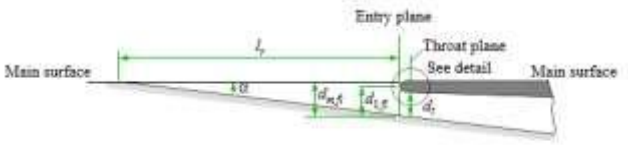

Fig. 4: Scheme and parameters of the inlet designed - ESDU, 1986.

The aircraft in question is being analyzed at the operational condition described in Table 1. Two different flight conditions were specified at this atmospheric condition: a) cruise condition at 2º AOA (Angle of attack); b) critical condition at 15º AOA, emulating a take-off flightpath.

Table.1: Design condition.

Parameters	Operational Condition
Speed	120 knots (61.73 m/s)
Angle of attack (AOA)	15º
Altitude	3000 ft (914.4 m)
Temperature	25ºC
Density	1.121 kg/m3
Pressure	90812 Pa

Using the ESDU with the objective of corroborating the CFD calculation, it is given the following variables with their respective values in Table 2, which are the mass flow, the boundary-layer thickness and the boundary-layer momentum thickness. Also, considering the throat aspect ratio and a ramp angle as depicted on Table 2. This NACA parameters leads to what was considered to be the minimum size of the flush inlet to provide air to the engine.

Table.2: Flush inlet design parameters.

ESDU parameters	Units
$\dot{m}$	0.016 slug/s
δ_h	0.1 ft
θ_0	0.01 ft
α_{ramp}	7º
w/dt	4

For a curved-divergent ramp inlet operating at maximum efficiency – Fig. 4, once given initial conditions to the problem it is calculated the mass flow parameter by equation (1):

$$\frac{\dot{m}}{\rho_0 V_0 \theta_0^2} = \frac{0{,}2330}{1{,}121x61{,}73x(0{,}003048)^2} = 363{,}209 \quad (1)$$

Knowing the throat aspect ratio, w/dt = 4, now by using the Fig. 20 (From ESDU 1986) for sizing a flush inlet to operate at maximum ram pressure efficiency, it was found:

$$\frac{\theta}{dt} = 0.075 \quad (2)$$

Now, it is known the value of the boundary layer momentum thickness, $\theta = 0.003048$. Then, it is possible to define dt = 0.0464m.
Further, having the value of dt, it is possible to get the width, from the throat aspect ratio:

w = dt× 4 = 0.16256 m

The lip is calculated assuming to be elliptically rounded with the lip length and thickness in the throat plane both equal to a quarter of the throat diameter in equation (2):

$$l = t = 0.25 \times dt \quad (3)$$
t =0.25 × (0.0464 m)

Thus,

t = 0.01016 m

The maximum external height of the inlet, d_{mfl} and the lip highlight height, d_{1fl}, determined in the inlet plane relative to the ramp floor, are calculated by equations (4) and (5):

$$d_{mfl} = dt + t - l_l \tan \propto = 0{,}04955 \quad (4)$$

$$d_{1fl} = dt + 0{,}5t - l_l \tan \propto = 0{,}044472 \quad (5)$$

The inlet capture area A1 is given through equation (6):

$$A1 = w \times d1fl \quad (6)$$
A1 = 0.0072294 m2

From Fig. 17 (ESDU, 1986) the maximum ram pressure efficiency, for a ramp angle equal to 7 and a throat aspect ratio of 4 is function of $\frac{\theta}{dt}$ which gives an efficiency of 0.82. Furthermore, the modified mass flow ratio at this value of efficiency is obtained interpolating on Figure 18 (ESDU, 1986) as Mm = 0.425, using equation (7) it can be found the following ratio:

$$\frac{\dot{m}}{\dot{m}_0} = 0{,}475 \frac{dt}{d_{1fl}} = 0{,}475 \frac{0{,}04064}{0{,}044472} = 0{,}4341 \quad (7)$$

In order to evaluate the total drag of this air-intake it was followed the diagram from Fig. 5. Then, the total inlet

https://dx.doi.org/10.22161/ijaers.4.5.7 *ISSN: 2349-6495(P) | 2456-1908(O)*

drag coefficient is given by Equation (8) and is divided in three components: ram drag, spillage drag and incremental drag correction.

$$C_{Dfl} = 2K_{fl}\frac{\dot{m}}{\dot{m}_0} + k_\alpha k_M k_{spfl} C'_{Dfl} + \Delta C_D \quad (8)$$

For the first component, the value of K_{fl} is calculated from equation (9) and according to the characteristics of the case, from Fig. 10a (ESDU), $k_\Psi = 1$:

$$K_{fl} = k_\Psi \left(\frac{\Psi_T}{\Psi_0}\right) \quad (9)$$

The Fig. 2 (ESDU) gives the momentum flow ratio with the respective values of δ/d_{1fl} and M. Finally, it is possible to achieve the ram drag component:

$$2k_\Psi \left(\frac{\Psi_T}{\Psi_0}\right)\frac{\dot{m}}{\dot{m}_0} = 0{,}7336$$

Now, for the spillage drag component which is the second term from equation (8), the factor k_α, k_M and k_{spfl} is obtained from Fig. 12, 13 and 14 (ESDU):

$$k_\alpha = 1$$
$$k_M = 1$$
$$k_{spfl} = 0{,}1793$$

The last term of the spillage drag coefficient is given by Fig. 11 (ESDU) for a curved-divergent ramp and as a function of $(d_{mfl} - d_{1fl})/l_l$. Acquiring these results the second component is obtained as it follows:

$$k_\alpha k_M k_{spfl} C'_{Dfl} = 0{,}0287$$

The incremental drag correction, third and last term from the inlet drag is calculated as a function of mass flow ratio from Fig. 15 (ESDU):

$$\Delta C_D = 0{,}0017$$

Then, knowing the values from each term of equation (8), the inlet drag is:

$$C_{Dfl} = 0.764$$

Therefore, using this simple semi-empirical approach it was possible to obtain the parameters for a design estimate for the flush inlet (NACA), which are specified in Fig. 6. A diagram showing the calculation steps is given in Fig. 7.

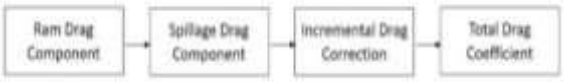

Fig. 5: Drag calculation diagram.

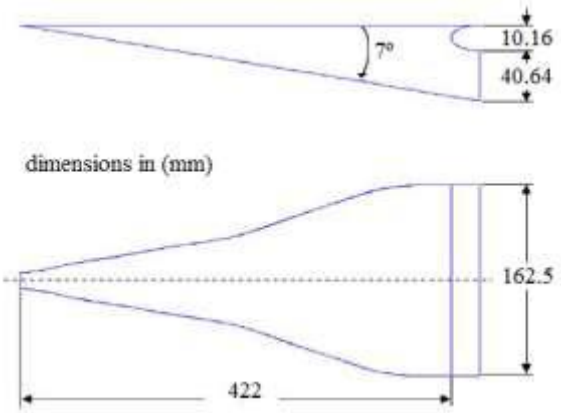

Fig. 6: NACA air inlet sizing.

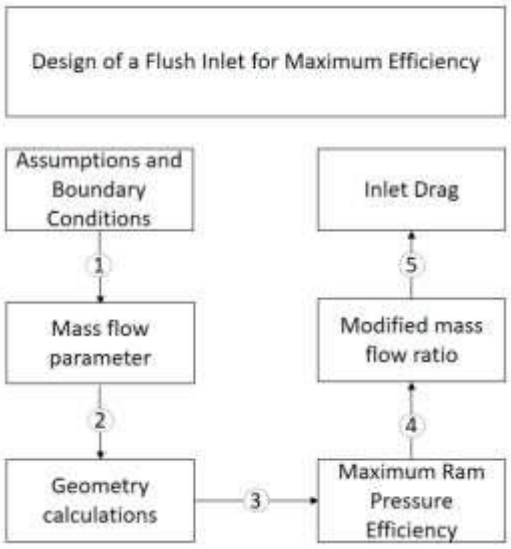

Fig. 7: Calculation diagram – summary of calculation procedure from ESDU, 1986.

Additional details for this semi-empirical method can be found in the ESDU document Item No. 86002 (ESDU, 1986).

IV. NUMERICAL METHOD

A Reynolds Averaged Navier-Stokes (RANS) approach was used in this work as a design tool and selection. The incompressible steady-state equations of motion were solved for different three dimensional domains with a NACA air inlet installed on it. The governing equations were solved with a second order accuracy through a Finite Volume formulation employed in the CFD++ software®. The final result was obtained by running 2000 iterations,

https://dx.doi.org/10.22161/ijaers.4.5.7 *ISSN: 2349-6495(P) | 2456-1908(O)*

or when the residuals dropped 5 orders of magnitude. For the turbulence modeling, the kω-SST (Shear Stress Transport, Menter (1993)) turbulence model was applied, based on experiences acquired in the past works with RANS equations applied to external flows with boundary layer detachment. The kω-SST model is a turbulence closure comprising a transport equation for the turbulent kinetic energy (k) and specific turbulence dissipation rate (ω). This model seems to provide reasonable results for external aerodynamics analysis and have been well documented in literature – Menter (1993), Menter (1994).

The CFD simulations were split in four parts:

a) An initial check and/or validation of the semi-empirical approach used to size the NACA air intake. In this case, the air inlet was mounted in a flat plate, with the imposition of an incoming uniform flow;

b) An incoming uniform flow based on the operating conditions of the aircraft, according to Table 1, was used to simulate only the flow over the aircraft's fuselage. The main purpose was to evaluate the velocity profile upon the air intake in the actual position along the aircraft's fuselage. This velocity profile will be used to adjust the flow simulation on step (a) of this approach;

c) An improvement of step (a) is performed by using the velocity profile evaluated in step (b) and imposing it on the NACA air inlet mounted in the flat plate;

d) Finally, the last step was to simulate the complete aircraft's fuselage with the NACA air inlet assembled on it, in its actual position and under the operational conditions of the airplane.

For brevity, only a summary of the computational domains and meshes for the flat plate and whole aircraft configuration will be not shown herein, in the next subsection.

4.1 Computational Domain

The initial validation was performed with the air inlet mounted in a flat plate. The computational domain for this configuration is shown in Fig. 8. The NACA air inlet was placed in the middle of the domain (50 Ln). A duct extension is inserted in this simulation in order to allow the flow to be completely developed inside the air intake, avoiding effect of the imposed boundary conditions. Details of the computational mesh are given in Fig. 9.

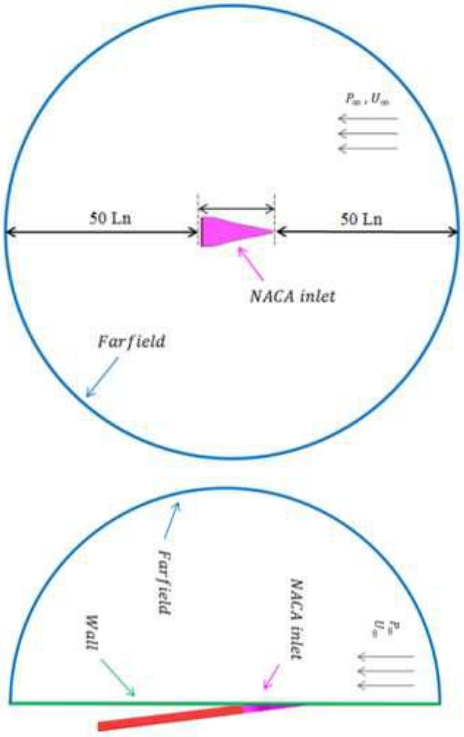

Fig. 8: Computational domain based on the length (Ln) of the NACA air inlet.

For the complete simulation, including the NACA assembled into the aircraft's fuselage, the computational domain is illustrated in Fig. 9. The size of the domains in x, y and z coordinates was selected based on previous studies (de Faria and Oliveira, 2002). The values shown below are considered suitable for such simulations and are used consistently through this whole work.

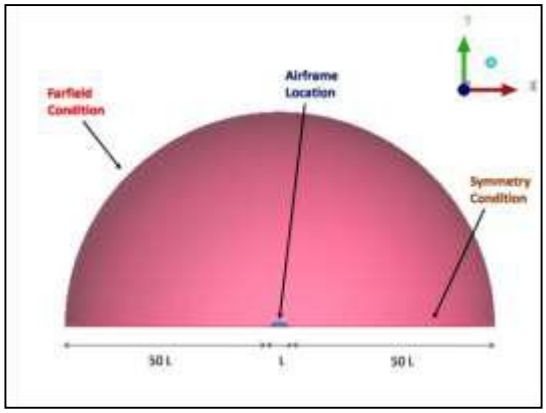

Fig. 9: Computational domain based on the Airframe's length (L).

4.2 Computational Meshes

The commercial software Ansys® IcemCFD was used to generate the unstructured meshes used in the simulations, Fig. 10 and 11 illustrate them. The discretization for the complete configuration consisted of an unstructured mesh with approximately 9 Million elements, with some refinements (density grids) on the desired regions of the

https://dx.doi.org/10.22161/ijaers.4.5.7 *ISSN: 2349-6495(P) | 2456-1908(O)*

flow. For the initial validation a mesh of approximately 4 Million elements was applied. As a control parameter the surface and volumetric mesh sizing around the air intake was kept approximately constant for both domains.

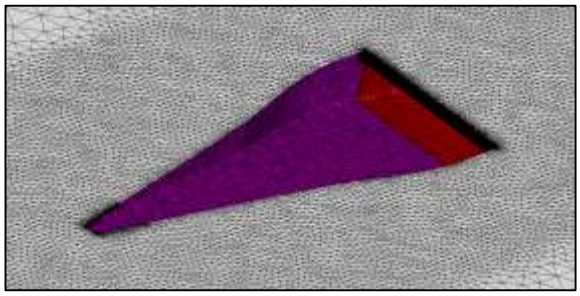

Fig.10: Mesh detail close to the NACA air intake – flat plate simulation.

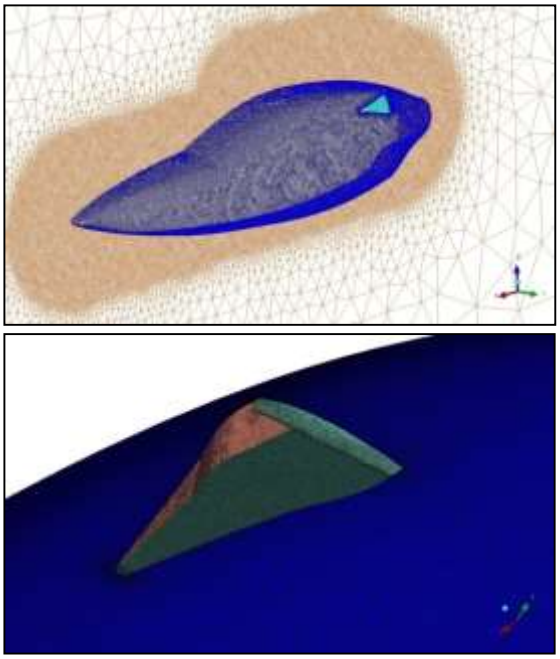

Fig. 11: Mesh details in different views – full simulation (NACA in the fuselage).

4.3 Boundary Conditions

Ambient atmospheric conditions were applied in both simulations with pressure and temperature set to 90812 Pa and 298.15 K, respectively. Walls were set to Non-slip and adiabatic boundaries. Since the outer boundary was placed far away from the body, farfield condition is assumed with minimum possibility of disturbing the internal domain solution. These set of boundary conditions are also illustrated on Fig. 7 and 8. For improving the incoming flow conditions in the flat plate simulation, a velocity profile was taken from the flow over the aircraft's fuselage and imposed in the farfield condition.

V. RESULTS AND DISCUSSION

The NACA efficiency is given by the relationship between the dynamic pressure at the throat and the dynamic pressure at infinity, according to Eq.(11):

$$\eta_{th} = \frac{Pt_{th} - Ps_{inf}}{Pt_{inf} - Ps_{inf}} \quad (11)$$

For the selected design, according to ESDU document Item No. 86002, the flush air inlet (NACA) throat area is 0.0072294 m^2. From the set of simulations performed in this work the achieved results for the inlet efficiencies are illustrated on Fig. 12, through the contours of dynamic pressure in the NACA's throat region. The global efficiency at the throat is calculated by summing the local (ηth) in each node at that location.

Fig.12(a) shows the result for the air inlet on a flat plate with a uniform flow condition. In this case, the efficiency is around 52%, showing a symmetric flow at the throat with the presence of a pair of vortices formed at the entry plane of the NACA. Despite the fact that these vortices may help the flow to go inside the air intake, in this case, the strength of them is reducing the efficiency. Moreover, the boundary layer flow is not the one developed at flight condition, since the imposition of a constant velocity is not really true. The effect of the flow profile already considering the real flight conditions of the airplane is then showed on Fig. 12(b). It can be noticed by the results the difference on hypothetic flow to a real one, efficiency fairly changes, without effects of attack angle. A great discrepancy is seen in the flow with a reduction in the strength of the vortices imposed at the NACA entry. In this case, the efficiency increased to nearly 83%. This relatively simple analysis allowed identifying the sensitiveness of this design to inlet flow conditions, especially in terms of the boundary layer's effect into the whole calculation. This interesting result showed that there is no option unless the complete simulation of the flow around the aircraft's fuselage with the NACA air intake installed on it.

Therefore, the efficiencies for the case of the air intake on the aircraft's fuselage are illustrated in Fig. 12(c) and (d). It can be seen all the effects of curvature that influence the flow stream to the air intake at the end portion of the fuselage. Two complete simulations were performed by analyzing the cruise condition at AOA around 2º(degrees) and the other in the critical condition with a 15° angle of attack (AOA). It may be noticed that in the cruise condition – Fig.12(c), there is little loss, the air inlet works very well in the recovery of pressure to the inside duct, due to the geometry of the aircraft which aids in the flow stream to the inlet air. Nevertheless, in critical condition due to influences of the high angle of attack the

https://dx.doi.org/10.22161/ijaers.4.5.7 *ISSN: 2349-6495(P) | 2456-1908(O)*

NACA air intake is seeing a disturbance into the flow resulting in a decrease in the value of efficiency. At cruise condition the efficiency is around 93% against nearly 63% at the critical condition – 15º AOA.

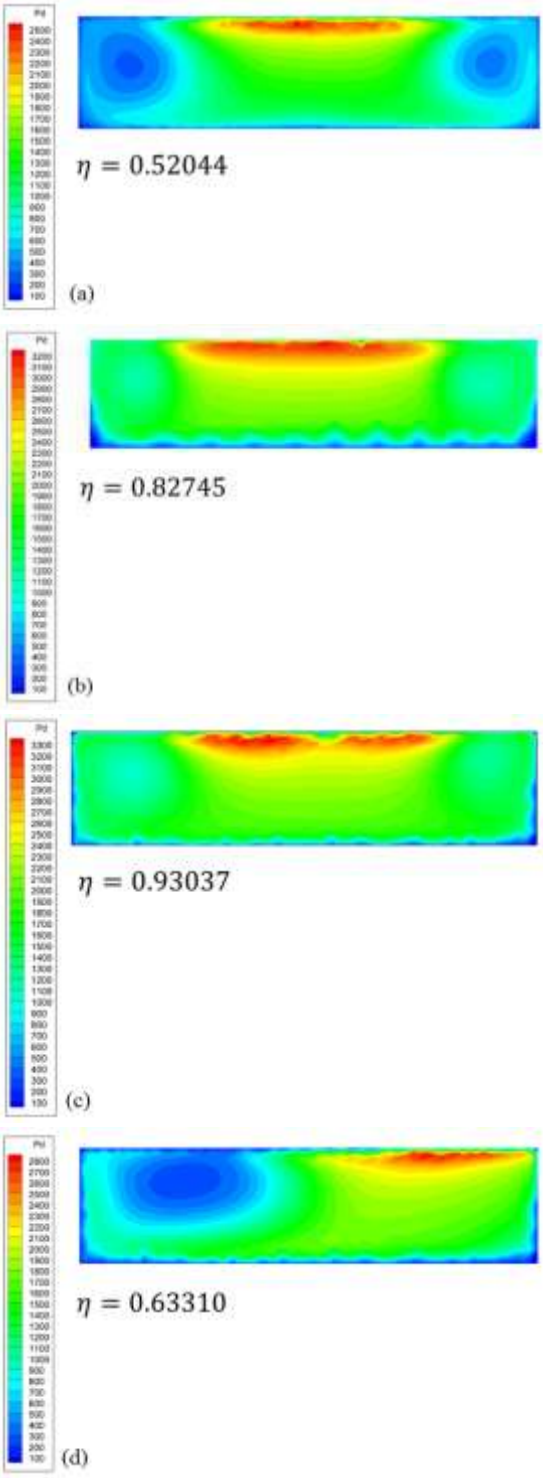

Fig. 12: Contours of dynamic pressure in the NACA's throat region: (a) NACA in the flat plate (uniform profile); (b) NACA in the flat plate (profile imposition); (c) NACA in cruising flight (0º AOA); (d) NACA in design operation (15º AOA).

It is also important to observe the flow pattern in the throat region for these two conditions. Again, in the cruise condition there is the appearance of the pair of vortices with low strength when compared with the flat plate simulations. The higher the intensity of strength of these vortices the low the efficiency is, as corroborated by Fig. 12(a), (b) and (c). At critical AOA condition, it is possible to see the asymmetry in the incoming flow at the inlet entry plane. In Fig. 6(d) it is possible to see only one vortex being formed and passing by the throat, although with higher strength. In this case, the efficiency decreased to 63%.

Fig. 13(a) and (b) allow a better understanding of the flow pattern around the aircraft's fuselage. At cruising condition, as seen on Fig.13 (a), the streamlines are rounding the fuselage of the entire aircraft and in the upper region of the aircraft; the flow is picked up with a little flow disturbance and interference. This led to a high efficiency for the NACA air intake around 83%. On the other hand, in Fig. 13 (b), representing the critical condition (AOA 15º), the streamlines are conform to the geometry of the fuselage only in the front part of the fuselage, featuring a more disordered and disturbed flow in the back portion, reducing the efficiency and pressure recovery via the air inlet located at that position.

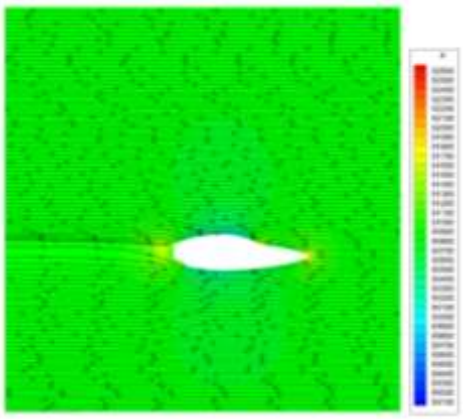

Cruising condition

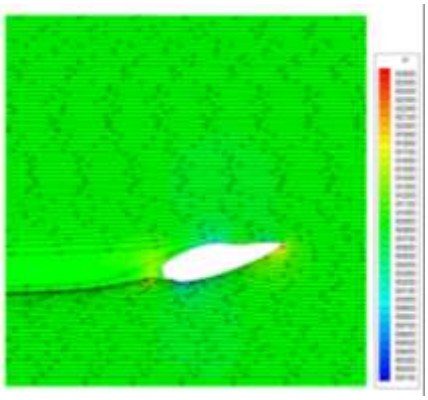

Critical condition AOA = 15º

Fig. 13: Streamlines for the flow around the aircraft's fuselage.

https://dx.doi.org/10.22161/ijaers.4.5.7 *ISSN: 2349-6495(P) | 2456-1908(O)*

By inspecting the Fig. 14, it is possible to see the pathlines, for the flow at cruise condition, entering the NACA air-intake. Part of the incoming flow is leaving the air-intake and becoming what is called "spillage" drag. The higher the spillage of the flow in the NACA air inlet the larger is the aerodynamic drag and lesser the air-intake efficiency.

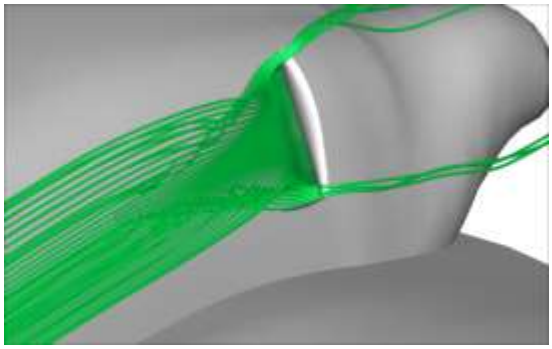

Fig. 14: Streamlines for the flow entering the NACA air-intake – cruise condition.

A closer look at the flow pattern incoming the NACA air inlet is provided in Fig. 15 (a) and (b).

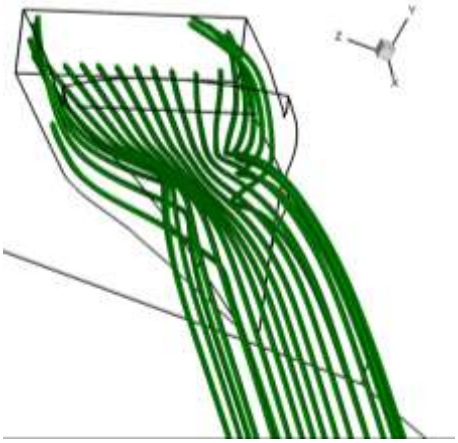

Cruising condition

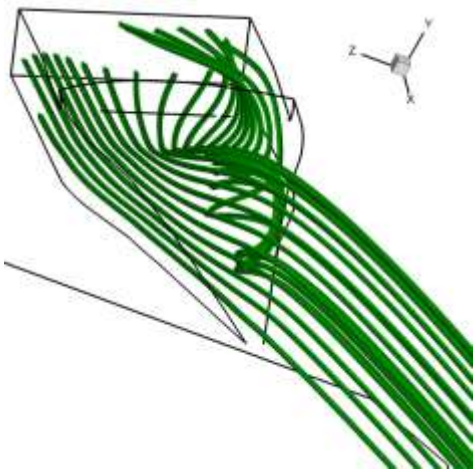

Critical condition AOA = 15º

Fig. 15: Streamlines incoming the Naca air inlet.

By analyzing the flow's pathlines, it is possible to see how the airflow behaves when captured by NACA. In the two conditions analyzed, the flow is much more orderly and permanent during the cruise, being possible to realize symmetry in the flow, while in critical condition, it is already asymmetric and totally disturbed.

Finally, by analyzing the data it is possible to affirm that the tested NACA air-intake gives reasonable efficiency in the flight conditions. The estimated drag for the component itself is given by the ESDU calculation and is around 0.764. It is important to emphasize that due to its flush geometry; the CFD drag prediction was not reasonable and it was not considered in this analysis.

The main concern in this design is to offer all mass flow rate inside the engine compartment, in order to cool it down. Based on the engine data and manufacturer's specification, additional semi-empirical and CFD simulations may be necessary to evaluate these quantities. The approach taken herein is quite acceptable in order to check new designs for the air-intake to be implemented in this aircraft. A further step will be the inclusion of different shapes of air inlets, such as scoops. In this case, a more refined analysis should take place in order to capture with more precision the drag force.

VI. CONCLUSION

A numerical investigation of the flow inside a NACA air intake was carried out for implementing a new configuration in a canard type aircraft. In such aircraft design the need for engine cooling is a very important aspect since the engine is placed at the back portion of the fuselage. This work described a semi-empirical approach coupled with CFD simulations procedures to design and select this NACA air inlet at different flight conditions. A set of numerical studies were performed with the air intakes mounted on a flat plate (theory check) and in the aircraft's fuselage. From the numerical computations, conducted using CFD++ with kω-SST turbulence model, it was concluded that the air inlet efficiency is highly dependent on the incoming flow and the boundary layer profile upstream the NACA air entry plane. In addition, the location of the NACA air intake in this aircraft's fuselage leads to efficiency of nearly 83% at cruise condition and around 63% in the critical condition at AOA approximately 15 degrees. Such conditions are restrictive in terms of mass flow rate through the engine compartment and a further study may apply to increase the size of the NACA air inlet or changing it to a SCOOP, at the price of increasing the aerodynamic drag of the whole aircraft. This study also indicates that the procedure used in this work is acceptable as an engineering tool, with relatively low cost, for design

https://dx.doi.org/10.22161/ijaers.4.5.7 *ISSN: 2349-6495(P) | 2456-1908(O)*

selection and indicative of design trends. Further work may also apply to improve the aircraft's configuration.

ACKNOWLEDGEMENTS

The authors acknowledge with gratitude the support of CPAERO – Experimental Aerodynamics Research Center at Federal University of Uberlândia for carrying out this work. The first author would like to thank Engº Pedro Ricardo Correa Souza for helping at the mesh and CFD simulations. Finally, we would like to thank the collaboration with the Brazilian Aircraft Factory (FABE).

REFERENCES

[1] DPW Drag Prediction Workshop, 2001. Applied aerodynamics conference, AIAA, Anahein, CA, USA.

[2] ESDU, 1968, The compressible two-dimensional turbulent boundary layer, both with and without heat transfer, on a smooth flat plate, with application to wedges, cylinders and cones, Item No. 68020 with amendment C, March 1988, Engineering Sciences Data Unit, London.

[3] ESDU, 1986, Drag and pressure recovery characteristics of auxiliary air inlets at subsonic speeds, Item No. 86002 with amendments A and B, July 1996, Engineering Sciences Data Unit, London.

[4] Hime, L. Estudo Numérico de Entradas de Ar para Aeronaves. Relatório PIBIC-CNPq, Departamento de Engenharia Mecânica, PUC-Rio, Rio de Janeiro, Julho 2004.

[5] http://forum.kerbalspaceprogram.com/threads/24551-Firespitter-propeller-plane-and-helicopter-parts-v7-1-(May-5th)-for-KSP-1-0/page38, Accessed on 01/06 at 17:20h.

[6] http://www.j-hangarspace.jp/, Accessed on 01/06 at 17:15h.

[7] Menter, F. R. (1993), "Zonal Two Equation k-ω Turbulence Models for Aerodynamic Flows", AIAA Paper 93-2906.

[8] Menter, F. R. (1994), "Two-Equation Eddy-Viscosity Turbulence Models for Engineering Applications", AIAA Journal, vol. 32, no 8. pp. 1598-1605.

[9] Nogueira de Faria, W.; Oliveira, G. L. Analise de Entradas de Ar Tipo NACA com Gerador de Vórtices. In 9th Brazilian Congress of Thermal Engineering and Sciences, ENCIT 2002, Caxambu-MG, Outubro, 2002.

[10] Rodriguez, D. L. A Multidisciplinary Optimization Method for Designing Inlets Using Complex Variables. In: 8th AIAA/USAF/NASA/ISSMO Symposium on Multidisciplinary Analysis and Optimization, September 2000.

[11] Taskinoglu, Ezgi S.; Knight, Doyle. Numerical Analysis of Submerged Inlets. In 20th AIAA Applied Aerodynamics Conference, St. Louis – Missouri, June 2002.